JACS
JOURNAL OF THE AMERICAN CHEMICAL SOCIETY

Communication

pubs.acs.org/JACS

Superhydrophobic Materials for Tunable Drug Release: Using Displacement of Air To Control Delivery Rates

Stefan T. Yohe,[†] Yolonda L. Colson,[‡] and Mark W. Grinstaff*,[†]

[†]Departments of Biomedical Engineering and Chemistry, Boston University, Boston, Massachusetts 02215, United States

[‡]Division of Thoracic Surgery, Department of Surgery, Brigham and Women's Hospital, Boston, Massachusetts 02215, United States

Supporting Information

ABSTRACT: We have prepared 3D superhydrophobic materials from biocompatible building blocks, where air acts as a barrier component in a porous electrospun mesh to control the rate at which drug is released. Specifically, we fabricated poly(ε-caprolactone) electrospun meshes containing poly(glycerol monostearate-*co*-ε-caprolactone) as a hydrophobic polymer dopant, which results in meshes with a high apparent contact angle. We demonstrate that the apparent contact angle of these meshes dictates the rate at which water penetrates into the porous network and displaces entrapped air. The addition of a model bioactive agent (SN-38) showed a release rate with a striking dependence on the apparent contact angle that can be explained by this displacement of air within the electrospun meshes. We further show that porous electrospun meshes with higher surface area can be prepared that release more slowly than control nonporous constructs. Finally, the entrapped air layer within superhydrophobic meshes is shown to be robust in the presence of serum, as drug-loaded meshes were efficacious against cancer cells in vitro for >60 days, thus demonstrating their applicability for long-term drug delivery.

Superhydrophobic surfaces are characterized as those with contact angles exceeding 150°. These textured nonwetting surfaces are readily found in nature (e.g., on plant leaves and the legs/wings of insects) and can be synthetically prepared via techniques such as templation, lithography, plasma treatment, and chemical deposition.[1] The phenomenon of a superhydrophobic surface is traditionally described using separate theories proposed in two landmark papers by Wenzel and Cassie. The Wenzel model characterizes a rough surface that is completely wetted in contact with a water droplet but shows an increase in contact angle over a chemically equivalent flat surface as a result of surface roughness.[2] Alternatively, the Cassie model describes a composite surface of a hydrophobic material and air.[3] In this model, the energetic favorability of a water droplet to wet a high-surface-area hydrophobic surface is so low that air remains entrapped under the droplet, markedly increasing the apparent contact angle of the droplet. The body of superhydrophobic surface research has established that both surface roughness and surface chemistry are required in order to produce materials with contact angles much greater than 120°, and examples of surfaces with apparent contact angles as high as 160° to approaching 180° have been reported.[4] In view of the unique property of superhydrophobicity, these surfaces have been actively investigated for a variety of applications where poor wettability is favorable, including antifouling, self-cleaning, and drag-reduction materials.[5] We hypothesized that 3D superhydrophobic materials may be ideal for drug delivery applications in which elution of an active agent over extended periods is required, since entrapped air within the material should act as a removable barrier component to slow drug release. Such a drug delivery system would be of clinical interest, for example, in pain management[6] and the prevention of tumor recurrence after surgical resection.[7] Here we describe the synthesis of superhydrophobic meshes from biocompatible building blocks; characterization of the meshes by contact angle, SEM, and AFM measurements; the controlled release of an entrapped agent, 7-ethyl-10-hydroxycamptothecin (SN-38), as a function of material contact angle; and the efficacy of SN-38-loaded meshes against a lung cancer cell line over an extended period. We also propose a mechanism of drug release based on the Wenzel and Cassie models.

For extended drug release, we needed to create both a superhydrophobic surface and a superhydrophobic bulk material (envisioned as multiple layers or a continuum of superhydrophobic surfaces) wherein entrapped air acts to delay the release from inner layers by slowing water penetration into the material. With this design requirement in mind, we selected the electrospinning[8] technique, which affords textured fibers overlaid on one another to give a bulk 3D porous mesh. We chose poly(ε-caprolactone) (PCL) (Figure 1A) as our base polymer for electrospinning, since it is biocompatible and widely used in polymeric medical devices, and we used poly(glycerol monostearate-*co*-ε-caprolactone) (1:4) (PGC-C18)[9] (Figure 1B) as a hydrophobic doping polymeric agent to be added to PCL to achieve the overall superhydrophobic state. This biocompatible copolymer of caproic acid and glycerol functionalized with stearic acid imparts a large hydrophobic effect from the stearic acid side chains.[9]

Specifically, PCL electrospun meshes were fabricated with varying amounts of PGC-C18 (0−50 wt %). The electrospinning processing conditions were adapted from previously published work for electrospinning of PCL [Table S1 in the Supporting Information (SI)].[10] The resulting meshes were 300 μm thick with an average fiber size of ∼7 μm. The wettability of the meshes was assessed using static contact angle measurements (Figure 2); the contact angles of electrospun

Received: November 28, 2011
Published: January 16, 2012

   dx.doi.org/10.1021/ja211148a | *J. Am. Chem.Soc.* 2012, 134, 2016−2019

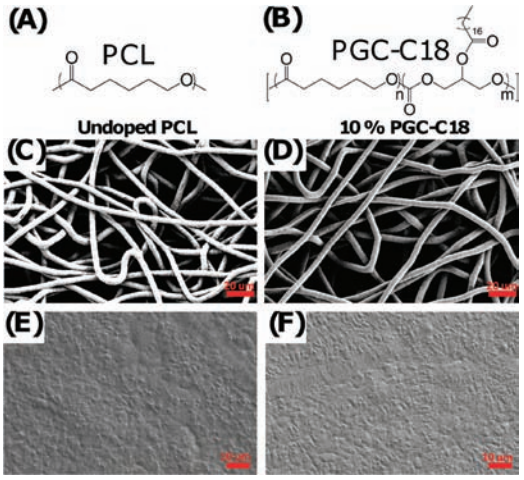

Figure 1. (A) PCL was used as the base polymer for fabrication of electrospun meshes and melted electrospun meshes. (B) PGC-C18 was used as the hydrophobic dopant in electrospun PCL meshes to decrease their wettability. (C) Electrospun PCL mesh with an average fiber size of 7.7 ± 1.2 μm. (D) 10% PGC-C18-doped electrospun PCL mesh with an average fiber size of 7.2 ± 1.4 μm. (E) A melted PCL mesh. (F) A melted 10% PGC-C18-doped electrospun PCL mesh.

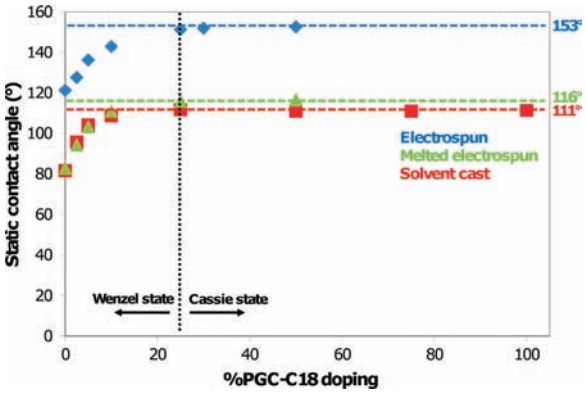

Figure 2. Contact angle measurements of electrospun meshes and chemically equivalent smooth surfaces as a function of PGC-C18 doping. The black dashed line indicates an approximate boundary for the ability to transition from the Cassie state to the Wenzel state.

PCL meshes doped with PGC-C18 asymptotically approached 153° with 50 wt % doping. As a control material, we also prepared melted electrospun meshes by heating the meshes at 80 °C for 1 min followed by quenching to collapse the porous structure on itself. This procedure was done quickly to prevent phase separation of PCL and PGC-C18, which was confirmed by differential scanning calorimetry (DSC) and consistent with their similar structures (Figure S1 in the SI). Studies of possible surface enrichment of the soft-chain hydrophobic pendant groups of PGC-C18 are ongoing.[11] Electrospun meshes and melted electrospun meshes for PCL and 10% PGC-C18-doped PCL were compared using SEM (Figure 1C–F), which showed that the melted meshes have comparably smooth surfaces. Additionally, the surface roughness of single electrospun fibers was quantified for PCL and PCL doped with 10% PGC-C18 using AFM. The electrospun fibers showed a finite surface roughness (rms roughness ~50 nm) (Figure S2) with consistent rms values between fibers with different PGC-C18 doping concentrations. This finite roughness indicates that both intra- and interfiber roughness may contribute to the high apparent contact angles. The melted electrospun meshes afforded a lower maximum contact angle of 116° with 50 wt % doping of PGC-C18 (Figure 2). Solvent-cast films of the polymers possessed contact angles similar to those of the melted electrospun meshes (Θ_{max} = 111°). Brunauer–Emmett–Teller (BET) surface area measurements on the electrospun and melted electrospun meshes using Kr showed that the electrospun meshes possessed at least 30 times more surface area than the melted counterparts (Table S1). To characterize further the superhydrophobic character of the PGC-C18-doped electrospun meshes, we performed a simple drop test to determine which meshes are in a metastable Cassie state.[12] We found that electrospun mesh surfaces with <25% PGC-C18 doping could be pushed into the stable Wenzel regime by dropping the water droplet used in the contact angle measurements from 2 feet. Electrospun meshes with >25% PGC-C18 doping could not be pushed into the Wenzel regime in this way, suggesting that 25% doping is an approximate boundary condition for the Wenzel-to-Cassie state transition.

With the above materials prepared, we were able to address our underlying hypothesis that air entrapped within the 3D fiber mesh would inhibit the penetration of water into the structure, thereby slowing the drug release, which occurs only at the material–water interface. Moreover, as these electrospun meshes possess a high surface area in comparison with their melted analogues, they enabled us to study high-surface-area materials exhibiting slow drug release. We chose SN-38 as the bioactive agent for the release studies because of its ease of detection and our previous experience.[13] SN-38 is the active form of the prodrug irinotecan, an antineoplastic used in the treatment of many cancers.[14] Electrospun meshes and melted electrospun meshes were kept completely submerged in pH 7.4 phosphate buffered saline (PBS) during release, and the release medium was changed regularly to maintain sink conditions for the drug (<10% drug solubility). Figure 3 shows the release profiles of porous electrospun meshes of PCL and 10%, 30%, and 50% PGC-C18-doped PCL relative to smooth melted electrospun surfaces. The electrospun PCL meshes and melted PCL meshes showed similar release rates, whereas the 10% PGC-C18-doped electrospun meshes exhibited significantly slower drug release relative to their melt controls. The melted 10% PGC-C18-doped PCL meshes stopped releasing SN-38 by 28 days, whereas the electrospun meshes continued to release SN-38 out to 70 days. The electrospun 10% PGC-C18-doped PCL mesh (i.e., the more porous, higher-surface-area material) released the drug more slowly. These results are consistent with the observation that the 10% PGC-C18-doped PCL electrospun mesh is in the metastable-Cassie state: the material starts with air entrapped within the porous structure, and over time, air is slowly displaced to create more area at the water–surface interface for SN-38 to be released. This finding provided impetus to evaluate a higher PGC-C18 doping concentration to determine whether an electrospun mesh with a more stable air layer could further slow the release of drug. The 30% and 50% PGC-C18-doped electrospun meshes showed only ~10% SN-38 release over 9 weeks.

Next, the presence and stability of entrapped air in the meshes was confirmed by several methods. When placed in PBS, the electrospun meshes remained at the surface, whereas the melted electrospun meshes sank immediately. Further, PCL meshes submerged in PBS for 70 days sank independently of applied force, whereas PGC-C18 doping maintained sufficient air content over this period to prevent sinking. PCL meshes

dx.doi.org/10.1021/ja211148a | J. Am. Chem.Soc. 2012, 134, 2016–2019

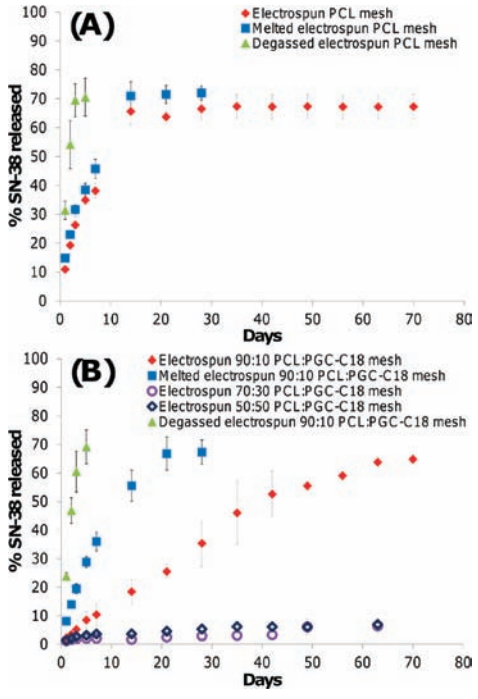

Figure 3. Release profiles comparing SN-38 release from (A) native, melted, and degassed PCL electrospun meshes and (B) native, melted, and degassed 10% PGC-C18-doped PCL electrospun meshes as well as meshes with PGC-C18 doping concentrations of 30 and 50 wt %.

could be forced to sink with brief sonication to remove the air. With an increase in the PGC-C18 doping concentration to 10%, treatment for a >100-fold longer sonication time was required to have the meshes sink. When 250 mL of water (~1.75 kPa) was placed above a 10% PGC-C18 mesh in a filtration setup, no water passed through after 1 month, while the same experimental setup for PCL showed water penetration after 3 days. To visualize the water penetration in the electrospun mesh directly, we imaged the meshes using X-ray computed tomography (CT) in an aqueous solution containing an iodinated contrast agent (see the SI). As shown in Figure 4,

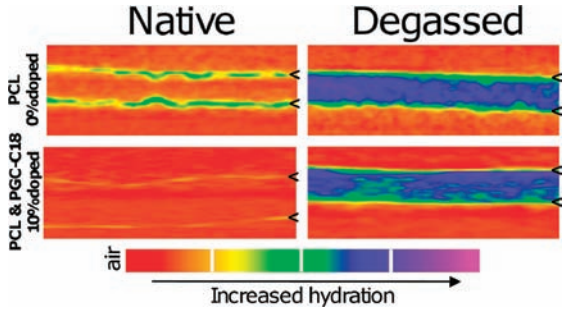

Figure 4. CT scans of native electrospun and degassed electrospun meshes with 0 or 10% PGC-C18 doping after incubation with the contrast agent Hexabrix for 2 h. Degassed meshes showed full water penetration, while native and melted meshes (not shown) exhibited only a low surface concentration of water. Tick marks define the top and bottom boundaries of the meshes.

CT images of degassed electrospun meshes showed complete penetration of water into the porous structure, whereas with native meshes, only surface penetration by water occurred (with less water at the surface of the 10% PGC-C18-doped PCL electrospun mesh), indicating that air remained within the mesh network. For comparison, melted meshes showed water at the surface, consistent with the lack of porosity within the structure. Finally, electrospun meshed that had been degassed via sonication released their drug at significantly higher rates. As shown in Figure 3B, 70% of the entrapped SN-38 was released within 7 days from sonicated 10% PGC-C18-doped PCL electrospun meshes, compared with 70 days of release for the native electrospun mesh.

All of the above data are consistent with the release rate being dependent on the rate at which water displaces air within the electrospun meshes. The 10% PGC-C18-doped PCL electrospun mesh is in the temporary, metastable Cassie state and shows slowed release relative to its chemically equivalent smooth melted surface. As shown pictorially in Figure 5, water

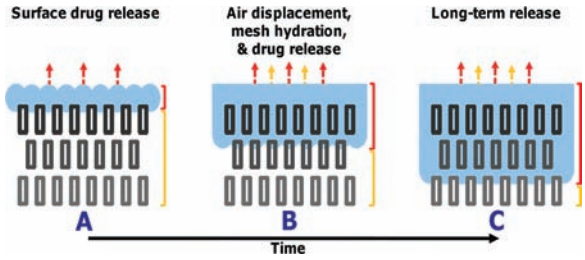

Figure 5. Proposed mechanism of a drug-eluting 3D superhydrophobic material.

penetrates into the structure in a time-dependent manner to displace entrapped air. Thus, air can act as a removable barrier component within the structure, effectively slowing the drug release by controlling the rate at which the internal polymer surface area is exposed to the release medium.

Next, we evaluated the SN-38-eluting electrospun meshes in a cytotoxicity assay in which serum albumin and other biological surfactants were present. It is well established that the addition of surfactants to superhydrophobic surfaces can decrease the surface tension of water and/or adsorb to the material surface to increasing the rate of wetting,[15] which would increase the rate of drug release. To test the effect of serum on the meshes, we first performed contact angle measurements on three mesh chemistries (0%, 10%, and 30% PGC-C18), where 10% serum was added to the applied droplet (Figure S4). Minimal changes in contact angle (<2°) were observed for all three meshes. We next incubated electrospun meshes in PBS containing 10% serum for 24 h to determine whether longer incubation times increased protein adsorption to promote wetting. No apparent contact angle was observed for the native PCL meshes, indicating that significant amounts of protein adsorption occurred to promote wetting. The 10% and 30% PGC-C18-doped PCL meshes exhibited only modest decreases (15° and 4°, respectively) in the apparent contact angle, showing that the entrapped air layer was present even in the presence of serum. Next, the SN-38-loaded meshes were incubated in serum-containing medium with Lewis lung carcinoma (LLC) cells (Figure 6). At a 1 wt % SN-38 concentration, both PCL and 10% PGC-C18-doped PCL meshes were cytotoxic to LLC cells for 90 days. No difference in the activities of these meshes was seen, as even a very small amount of released SN-38 is cytotoxic because of the low IC_{50} of SN-38 (~8 ng/mL). Decreasing the SN-38 loading 10-fold afforded a significant difference between the PCL and 10%

dx.doi.org/10.1021/ja211148a | J. Am. Chem.Soc. 2012, 134, 2016–2019

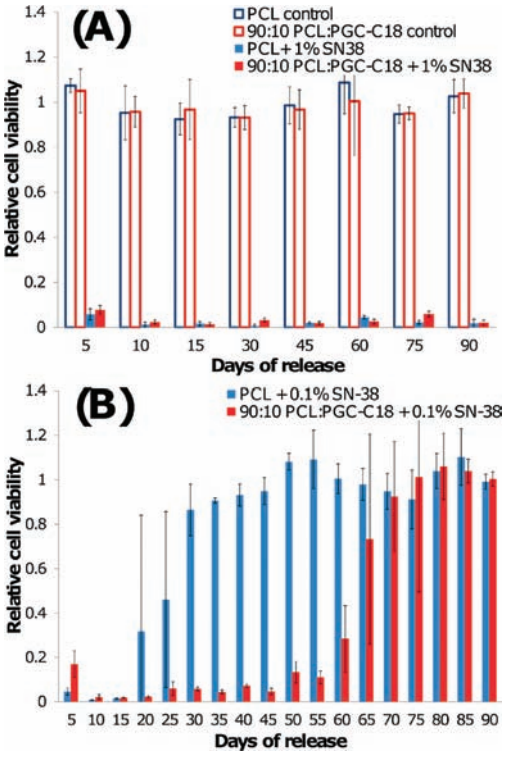

Figure 6. Cytotoxicity profiles upon incubation of LLC cells with PCL meshes and 10% PGC-C18-doped PCL meshes containing (A) 1 wt % or (B) 0.1 wt % SN-38. Both chemistries effectively treated LLC cells for 90 days at 1 wt % SN-38. When the SN-38 concentration was decreased 10-fold, a significant difference in performance was observed, as the PCL meshes were cytotoxic to LLC cells for 25 days while the 10% PGC-C18-doped PCL meshes showed cytotoxicity for 65 days. Unloaded meshes were not cytotoxic to cells.

PGC-C18-doped PCL meshes. The former were cytotoxic for 25 days, whereas the latter were cytotoxic for 65 days. Unloaded meshes were not toxic to cells.

In summary, 3D superhydrophobic meshes composed of hydroxycaproic acid, glycerol, and stearic acid can readily be fabricated using the electrospinning technique. The resulting meshes have high surface area and possess apparent contact angles as high as 153°. When the electrospun meshes are loaded with an anticancer agent (SN-38), the high apparent contact angle restricts water penetration and slows displacement of air from the high porosity meshes, thus slowing SN-38 release into the aqueous solution. The release rates of SN-38 are strikingly different than those of the melted, nonporous analogues as well as the degassed electrospun controls. In the presence of serum, the SN-38-loaded 10% PGC-C18-doped PCL mesh is cytotoxic to LLC cells in vitro and performs for an extended time period. The concepts underlying our results will assist others in preparing new materials for drug delivery,[16] including translation to other polymers and drug compositions, as long as the following design specifications are maintained: (1) the processing technique must allow the production of a porous, bulk material; (2) the produced constructs must have sufficient thickness to promote slow, controlled water penetration; and (3) the constructs must have a high enough apparent contact angle to entrap air within the structure and provide a sufficient barrier to slow the penetration of water.

■ ASSOCIATED CONTENT

Supporting Information

Experimental design, additional mesh characterization, and contact angles with serum addition. This material is available free of charge via the Internet at http://pubs.acs.org.

■ AUTHOR INFORMATION

Corresponding Author

mgrin@bu.edu

Notes

The authors declare no competing financial interest.

■ ACKNOWLEDGMENTS

This work was supported in part by BU, CIMIT, the Coulter Foundation, and NIH (R01CA149561).

■ REFERENCES

(1) Li, X.-M.; Reinhoudt, D.; Crego-Calama, M. *Chem. Soc. Rev.* **2007**, *36*, 1350.
(2) Wenzel, R. N. *J. Ind. Eng. Chem.* **1936**, *28*, 988.
(3) Cassie, A. B. D.; Baxter, S. *Trans. Faraday Soc.* **1944**, *40*, 546.
(4) (a) Shieh, J.; Hou, F. J.; Chen, Y. C.; Chen, H. M.; Yang, S. P.; Cheng, C. C.; Chen, H. L. *Adv. Mater.* **2010**, *22*, 597. (b) Tuteja, A.; Choi, W.; Ma, M.; Mabry, J. M.; Mazzella, S. A.; Rutledge, G. C.; McKinley, G. H.; Cohen, R. E. *Science* **2007**, *318*, 1618.
(5) (a) Genzer, J.; Efimenko, K. *Biofouling* **2006**, *22*, 339. (b) Nakajima, A.; Hashimoto, K.; Watanabe, T. *Monatsh. Chem.* **2001**, *132*, 31. (c) Nosonovsky, M.; Bhushan, B. *Curr. Opin. Colloid Interface Sci.* **2009**, *14*, 270.
(6) Al Malyan, M.; Becchi, C.; Nikkola, L.; Viitanen, P.; Boncinelli, S.; Chiellini, F.; Ashammakhi, N. *J. Craniofacial Surg.* **2006**, *17*, 302.
(7) Wolinsky, J. B.; Colson, Y. L.; Grinstaff, M. W. *J. Controlled Release* **2011**, in press.
(8) (a) Ma, M.; Hill, R. M.; Rutledge, G. C. *J. Adhes. Sci. Technol.* **2008**, *22*, 1799. (b) Agarwal, S.; Wendorff, J. H.; Greiner, A. *Polymer* **2008**, *49*, 5603. (c) Reneker, D. H.; Yarin, A. L. *Polymer* **2008**, *49*, 2387.
(9) Wolinsky, J. B.; Ray, W. C. III; Colson, Y. L.; Grinstaff, M. W. *Macromolecules* **2007**, *40*, 7065.
(10) Pham, Q. P.; Sharma, U.; Mikos, A. G. *Biomacromolecules* **2006**, *7*, 2796.
(11) (a) Yoon, S. C.; Ratner, B. D. *Macromolecules* **1986**, *19*, 1068. (b) Thomas, H. R.; O'Malley, J. J. *Macromolecules* **1979**, *12*, 323.
(12) Tsai, P.; Pacheco, S.; Pirat, C.; Lefferts, L.; Lohse, D. *Langmuir* **2009**, *25*, 12293.
(13) (a) Wolinsky, J. B.; Liu, R.; Walpole, J.; Chirieac, L. R.; Colson, Y. L.; Grinstaff, M. W. *J. Controlled Release* **2010**, *144*, 280. (b) Morgan, M. T.; Nakanishi, Y.; Kroll, D. J.; Griset, A. P.; Carnahan, M. A.; Wathier, M.; Oberlies, N. H.; Manikumar, G.; Wani, M. C.; Grinstaff, M. W. *Cancer Res.* **2006**, *66*, 11913.
(14) Mathijssen, R. H. J.; Van Alphen, R. J.; Verweij, J.; Loos, W. J.; Nooter, K.; Stoter, G.; Sparreboom, A. *Clin. Cancer Res.* **2001**, *7*, 2182.
(15) (a) Mohammadi, R.; Wassink, J.; Amirfazli, A. *Langmuir* **2004**, *20*, 9657. (b) Ferrari, M.; Ravera, F.; Rao, S.; Liggieri, L. *Appl. Phys. Lett.* **2006**, *89*, No. 053104.
(16) (a) Lee, C. C.; MacKay, J. A.; Fréchet, J. M. J.; Szoka, F. C. *Nat. Biotechnol.* **2005**, *23*, 1517. (b) Wu, P.; Grainger, D. W. *Biomaterials* **2006**, *27*, 2450. (c) Langer, R.; Tirrell, D. A. *Nature* **2004**, *428*, 487. (d) Kopecek, J.; Yang, J. Y. *Polym. Int.* **2007**, *56*, 1078. (e) Hoare, T. R.; Kohane, D. S. *Polymer* **2008**, *49*, 1993. (f) Wolinsky, J. B.; Grinstaff, M. W. *Adv. Drug Delivery Rev.* **2008**, *60*, 1037. (g) Davis, M. E.; Chen, Z.; Shin, D. M. *Nat. Rev. Drug Discovery* **2008**, *7*, 771. (h) Rothenfluh, D. A.; Hubbell, J. A. *Integr. Biol.* **2009**, *7*, 446. (i) Kim, S.; Kim, J.-H.; Jeon, O.; Kwon, I. C.; Park, K. *Eur. J. Pharm. Biopharm.* **2009**, *71*, 420.